

Localization of Polymers in Random Media: Analogy with Quantum Particles in Disorder

Yadin Y. Goldschmidt ^a and Yohannes Shiferaw ^b

^aUniversity of Pittsburgh, Department of Physics, Pittsburgh, Pennsylvania 15260.

^bUniversity of California, Department of Medicine and Cardiology, Los Angeles, CA 90095-1679.

1. Introduction

Polymers are very long chain-like macromolecules that play an important role in a wide variety of physical systems. Many of the materials that we encounter in our every day lives, such as plastics and rubber, are essentially a mesh like structure of polymers. In biology, polymers also play a central role, as many biological molecules, such as DNA, have a long chain-like structure. In this chapter we focus on the equilibrium statistical mechanics of a single polymer chain immersed in a quenched random medium. For example, a chain that is free to move in a porous material, such as a sponge or a complicated gel network. This problem is relevant to a number of technologically important processes, such as filtration [1, 2], gel permeation chromatography [3, 4], and the transport of polymers through porous membranes [5]. Here, we will not address these practical issues, but rather, give an overview of the theoretical aspects of the problem.

In this chapter we present analytical and numerical results on the conformational statistics of polymers in quenched random media. We first consider the problem of a Gaussian polymer chain in a random potential characterized by short ranged correlations. This simplified mathematical model of a real polymer is tackled analytically using the replica method, and also via a mapping to the equivalent problem of a quantum particle in a random potential. Here, we will focus on the statistical properties of a long polymer chain, where the free-energy landscape is complex and possesses many meta-stable states. Using the path integral mapping between the partition function of a Gaussian polymer chain and the imaginary time Schrödinger equation, we show that the glassy phase can be understood in terms of the localized eigenfunctions of the Schrödinger equation with a random potential. Furthermore, we show that the glassy behavior can also be described analytically by a one-step replica-symmetry-breaking (RSB) solution. We explore the connection between the replica solution and the eigenfunctions of the Schrödinger equation, and show that the one-step RSB solution can be interpreted in terms of the dominance of localized tail states.

We proceed to investigate the more realistic case of a chain immersed in a sea of hard obstacles that are randomly distributed in space. Prior to our work it was often assumed in

the literature that this problem is equivalent to the random potential problem. Using Flory type free energy arguments we elucidate the similarities and differences between this case and that of a random potential with short ranged correlations. In particular, we show that the dependence of the polymer size on chain length can exhibit three possible scaling regimes depending on the system size.

Finally, we introduce a more realistic model that includes a self-avoiding interaction between monomers of the polymer chain. We show that in the limit of a very long chain, and when the self-avoiding interaction is weak, the equilibrium chain conformation consists of many blobs with connecting segments. These blobs are situated in regions of low average potential, in the random potential case, or in a region of low density of obstacles in the random obstacles case. We also show that as the strength of the self-avoiding interaction is increased relative to the strength of the random potential, the polymer chain undergoes a localization-delocalization transition, where the chain is no longer bound to a particular region of the medium but can easily wander around under the influence of a small perturbation.

2. The statistics of a Gaussian chain in a random potential

2.1. Path integral formalism

A polymer is a collection of molecules, called monomers, which interact with each other to form a long flexible chain. For example, a typical polymer like polyethylene consists of a chain of roughly 10^5 CH_2 molecules. The large number of monomers allows for a statistical description of macroscopic properties which are independent of details on the monomer scale. The simplest mathematical model of a polymer chain is referred to as the Gaussian chain [6]. In this model the polymer is described by a position d -dimensional vector $\mathbf{R}(u)$, where u is a continuous variable which satisfies $0 < u < L$, and which runs along the contour of a chain with length L . The probability of finding a conformation $\mathbf{R}(u)$ is given by

$$P[\mathbf{R}(u)] = \mathcal{N} \exp \left[-\frac{d}{2b^2} \int_0^L du \left(\frac{d\mathbf{R}(u)}{du} \right)^2 \right], \quad (1)$$

where \mathcal{N} is a normalization constant, and where b is the average bond length. In this description the self-avoiding interaction of the chain with itself is not taken into account, and in the absence of an external potential the conformation of the chain resembles the trajectory of a random walker with a mean step b . Thus, the average end-to-end distance of the chain satisfies

$$\langle (\mathbf{R}(L) - \mathbf{R}(0))^2 \rangle = L b^2. \quad (2)$$

The conformational statistics of a polymer chain will change if the chain is placed in a random environment. We can model the effect of the random environment by introducing an interaction energy

$$E_{int}[\mathbf{R}(u)] = \int_0^L du V(\mathbf{R}(u)), \quad (3)$$

where $V(\mathbf{R})$ is the potential energy of a monomer at the position \mathbf{R} due to the environment. The potential function $V(\mathbf{R})$ will depend on the type of random medium that is being studied, and will be discussed in more detail later. The conformational probability is now

$$P[\mathbf{R}(u)] = \mathcal{N} \exp \left[-\frac{d}{2b^2} \int_0^L du \left(\frac{d\mathbf{R}(u)}{du} \right)^2 - \beta \int_0^L du V(\mathbf{R}(u)) \right], \quad (4)$$

where we multiplied the free Gaussian conformational probability with the Boltzmann factor $\exp(-\beta E_{int}[\mathbf{R}(u)])$, with $\beta = 1/kT$. Given the conformational probability we can write the partition sum (Green's function) for the paths of length L that go from \mathbf{R} to \mathbf{R}' as

$$Z(\mathbf{R}, \mathbf{R}'; L) = \int_{\mathbf{R}(0)=\mathbf{R}}^{\mathbf{R}(L)=\mathbf{R}'} [d\mathbf{R}(u)] \exp(-\beta H), \quad (5)$$

where

$$H = \int_0^L du \left[\frac{M}{2} \left(\frac{d\mathbf{R}(u)}{du} \right)^2 + V(\mathbf{R}(u)) \right], \quad (6)$$

and where $M = d/(\beta b^2)$. All the statistical properties of the polymer chain can be derived from this partition sum.

In this chapter we will also consider the effects of the volume of the random medium i.e. the system size. In order to incorporate this effect in the partition function we include a harmonic term

$$V(\mathbf{R}(u)) \rightarrow V(\mathbf{R}(u)) + \frac{\mu}{2} \mathbf{R}^2(u), \quad (7)$$

where the coefficient μ will be a measure of the available volume to the polymer (A larger μ implies a smaller system volume). The confining well is also important to ensure that the model is well defined, since it turns out that certain equilibrium properties of the polymer diverge in the infinite volume limit ($\mu \rightarrow 0$).

A quenched random medium, such as a rough surface or a frozen gel network, is a complex structure that can in principle be modelled by a complicated potential function $V(\mathbf{R})$. However, we will not be interested in the physical properties of a polymer chain immersed in a specific environment, but rather in an ensemble of similar environments. Hence, we will have to specify instead the probability distribution of the random potential $V(\mathbf{R})$. Here, we will consider random potentials that are taken from a Gaussian distribution defined by

$$\langle V(\mathbf{R}) \rangle = 0, \quad \langle V(\mathbf{R})V(\mathbf{R}') \rangle = f((\mathbf{R} - \mathbf{R}')^2). \quad (8)$$

In particular we will consider a correlation function of the form

$$f((\mathbf{R} - \mathbf{R}')^2) = \frac{g}{(\pi\xi^2)^{d/2}} \exp(-(\mathbf{R} - \mathbf{R}')^2/\xi^2), \quad (9)$$

where g determines the strength of the disorder and the parameter ξ conveniently controls the correlation range of the random potential. Here, we will consider only the case of short-range correlations, where ξ is much smaller than the system size.

All the statistical properties of the polymer will depend on the partition sum. For instance, the average end-to-end distance of a polymer chain that is free to move is given by

$$\overline{\langle \mathbf{R}_F^2(L) \rangle} = \overline{\left(\frac{\int d\mathbf{R}d\mathbf{R}'(\mathbf{R} - \mathbf{R}')^2 Z(\mathbf{R}, \mathbf{R}'; L)}{\int d\mathbf{R}d\mathbf{R}' Z(\mathbf{R}, \mathbf{R}'; L)} \right)}, \quad (10)$$

where the over-bar stands for the average of the ratio over realizations of the random potential. This average is referred to as a quenched average, as opposed to an annealed average, where the numerator and denominator are averaged independently. In some previous studies it has been argued that for the mean end-to-end distance, as defined in Eq. 10, one can replace the quenched average by the more analytically tractable annealed average. However, this replacement can be justified only when the system size is strictly infinite, since only in that limit can the polymer sample all of space and find the most favorable potential well that will be similar to its environment in the annealed case. The main problem with this approach is that in practice we always deal with finite-size systems, and it is not always easy to assess how big the system size has to be so that the annealed average is a good approximation to the quenched average. In addition, the time it takes the chain to sample a large volume is exceedingly long and unreachable over a reasonable experimental time.

Before ending this section we would like to point out the relationship between the statistical properties of a polymer chain and a variety of other physical problems. The partition sum, as written in Eq. (5), is in the form of a path integral over all possible chain conformations. Since many physical problems can be formulated in terms of path integrals, we can map the problem of a Gaussian polymer in a random media to a wide variety of seemingly unrelated problems. First, we can map the partition sum of a polymer chain to the density matrix of a quantum particle. The mapping [7, 8] is given by

$$\beta \rightarrow 1/\hbar, \quad L \rightarrow \beta\hbar. \quad (11)$$

The density matrix of a quantum particle at inverse temperature β is then related to the partition function of the polymer as

$$\rho(\mathbf{R}, \mathbf{R}'; \beta) = Z(\mathbf{R}, \mathbf{R}'; L = \beta\hbar, \beta = 1/\hbar). \quad (12)$$

The monomer label u is now interpreted as the Trotter (imaginary) time, and M as the mass of the quantum particle. The density matrix is relevant to the equilibrium statistical mechanics of a quantum particle, such as an electron in a dirty metal.

The polymer partition sum for a Gaussian chain in random potential can also be mapped into the partition sum of a flux-line in type-II superconductors in the presence of columnar disorder [9, 10]. Here, $\mathbf{R}(u)$ is the transverse displacement of the flux-line (or vortex). The variable u is interpreted as the distance along the z -axis (direction of the magnetic field), and the variable M corresponds to the line tension of the flux-line. Thus a flux-line in three dimensions propagating along the z -direction maps into a polymer in two spatial

| Polymer chain | Quantum particle | Flux line |
|--------------------------------------|----------------------------|---------------------------------------|
| u (monomer label) | τ (imaginary time) | z (plane label) |
| β | $1/\hbar$ | β |
| L (chain length) | $\hbar\beta$ | L_z (distance along z-direction) |
| $d/\beta b^2$ (b =bond length) | m (mass) | ϵ_ℓ (line tension) |

Table 1

The relationship between different physical systems.

dimensions (its projection onto the plane), and the columnar disorder maps into point disorder. Although, in the case of several flux-lines there is a repulsive electromagnetic interaction among them which is not present for polymer chains. In Table 1 we have summarized the relationships between a polymer chain, a quantum particle, and a flux-line in a superconductor.

Finally, we can also map the polymer problem to the problem of diffusion in a random catalytic environment [11, 12]. This process describes, for instance, auto-catalytic chemical reactions in a disordered background, or the spreading of a population with a growth rate that depends on local random conditions. If we make the replacements

$$\frac{1}{2M\beta} \rightarrow D, \quad \beta V(\mathbf{R}) \rightarrow -U(\mathbf{R}), \quad L \rightarrow t \quad (13)$$

where D is the diffusion constant, and $U(\mathbf{R})$ is the growth rate (or reaction rate) at position \mathbf{R} , and t is the time. Then $Z(\mathbf{R}', \mathbf{R}; t)$ gives the concentration of the constituents at position \mathbf{R}' at time t , given a delta function concentration concentrated at \mathbf{R} at time $t = 0$.

2.2. Flory arguments

A remarkably fruitful approach to the statistics of polymers is via simple and intuitive free energy arguments. This approach was used with great success by Cates and Ball [13] to derive the essential scaling properties of a polymer in a random potential. Here, we reproduce their beautiful intuitive arguments in order to elucidate the effect of a finite volume on the behavior of an untethered free chain in a random potential. First, Cates and Ball argue that a Gaussian chain situated in an infinite random medium is always collapsed in the long-chain limit. Their argument goes as follows: Consider a white-noise random potential $V(x)$ of zero mean whose probability distribution is

$$P(V(x)) \propto g^{-1/2} \exp(-V^2/2g). \quad (14)$$

If we now coarse-grain the medium and denote by \bar{V} the average value of the potential over some region of volume Ω , then the coarse-grained potential will have the distribution

$$P_\Omega(\bar{V}) \propto (g/\Omega)^{-1/2} \exp(-\Omega\bar{V}^2/2g). \quad (15)$$

Now, consider a polymer chain situated in the random potential, and assume that it shrinks into a volume Ω corresponding to a place where the mean potential \bar{V} takes on a lower value than usual. In this situation the free energy of the chain is crudely estimated to be (neglecting all numerical factors):

$$F(\Omega, \bar{V}) = L/R^2 + L\bar{V} + \Omega\bar{V}^2/2g. \quad (16)$$

Here, L is the length of the chain (number of monomers), R is the radius of gyration (or end-to-end distance) and the volume Ω is related to R via $\Omega \sim R^d$ in d -spatial dimensions. The first term on the r.h.s. is an estimate of the free energy of a long chain confined to a region of size R in the absence of an external potential (see e.g. [14], Eq. I.12). The second term is just the potential energy of the chain in the random potential of strength \bar{V} . The third term arises from the chance of incurring a random potential of strength \bar{V} . The quantity $\ln P(\bar{V})$ gives an associated effective entropy for the system. Minimizing this free energy over both \bar{V} and Ω determines the lowest free energy configuration. Minimizing with respect to \bar{V} yields $\bar{V} = -Lg/\Omega$. Substituting in F gives:

$$F(R) = \frac{L}{R^2} - \frac{L^2g}{2R^d}. \quad (17)$$

This shows that for any $d \geq 2$, $F \rightarrow -\infty$ as $R \rightarrow 0$. Thus, the mean size of the chain is zero, or in the presence of a cutoff, the size of one monomer i.e.

$$R \sim 1, \quad d \geq 2. \quad (18)$$

For $d < 2$, the free energy has a minimum for

$$R \sim (Lg)^{1/(d-2)}, \quad d < 2, \quad (19)$$

which in the long chain limit ($L \geq 1/g$) cuts off again at $R \sim 1$. These results are the same as those for the case of an annealed potential that is able to adjust locally to lower the free energy of the system. The reason is that for an infinite system containing a finite (even though long) chain, space can be divided into regions containing different realizations of the potential, and the chain can sample all of these to find an environment arbitrarily similar to that which would occur in the annealed situation.

These results stand in contrast to the replica calculation of Edwards and Muthukumar (EM) [15], who found that for a long chain

$$R \sim g^{-1/(4-d)}, \quad d < 4 \quad (20)$$

when $g^{2/(4-d)}L \rightarrow \infty$, whereas $R \sim L^{1/2}$ when $g^{2/(4-d)}L \rightarrow 0$. Note that the result (20) is independent of L as opposed to Eq. (19). To reconcile the two apparently different results, Cates and Ball argue that the quenched case is different from the annealed case only for the case when the medium has a *finite* volume \mathcal{V} . In a finite box, arbitrarily deep potential minima are not present. Instead the most negative \bar{V} averaged over a region of volume $\Omega \ll \mathcal{V}$ occupied by the chain, is approximately (keeping only leading terms

in the volume V) given by solving the equation (the l.h.s. of which represents the area under the tail of the distribution)

$$\int_{-\infty}^{\bar{V}} dy P_{\Omega}(y) \simeq \frac{\Omega}{\mathcal{V}}, \quad (21)$$

which yields

$$\bar{V} = -\sqrt{\frac{g \ln \mathcal{V}}{\Omega}}. \quad (22)$$

This expression when plugged into Eq. (16) leads to (note that the last term in (16) just becomes a constant independent of R)

$$F(R) = \frac{L}{R^2} - L\sqrt{\frac{g \ln \mathcal{V}}{R^d}}. \quad (23)$$

When this free energy is minimized with respect to R it gives rise to

$$R \sim (g \ln \mathcal{V})^{-1/(4-d)}, \quad d < 4. \quad (24)$$

Using this value the binding energy per monomer becomes

$$U_{bind}/L = (g \ln \mathcal{V})^{2/(4-d)}. \quad (25)$$

For the polymer to be localized its total binding energy has to be greater than the translational entropy $\ln \mathcal{V}$, which is always satisfied for $2 < d < 4$ when L or \mathcal{V} are large (and for $d = 2$ when L is large).

2.3. The relation to the localization of a quantum particle

In order to understand the conformational statistics of a Gaussian chain in a random potential, we map the partition sum to an imaginary time Schrödinger equation. This mapping (see Ref. [7] Eqs. (3.12)-(3.18)) is given by

$$Z(\mathbf{R}, \mathbf{R}'; L) = \int_{\mathbf{R}(0)=\mathbf{R}'}^{\mathbf{R}(L)=\mathbf{R}} [d\mathbf{R}(u)] \exp(-\beta H[\mathbf{R}(u)]) = \langle \mathbf{R} | \exp(-\beta L \hat{H}) | \mathbf{R}' \rangle, \quad (26)$$

where

$$\hat{H} = -\frac{1}{2M\beta^2} \frac{\partial^2}{\partial \hat{\mathbf{R}}^2} + \frac{\mu}{2} \hat{\mathbf{R}}^2 + V(\hat{\mathbf{R}}). \quad (27)$$

So for a given realization of the random potential the polymer partition sum can be expressed as a matrix element of the imaginary-time evolution operator. The matrix elements can be expanded in eigenfunctions of the Hamiltonian operator to yield

$$\langle \mathbf{R} | \exp(-\beta L \hat{H}) | \mathbf{R}' \rangle = \sum_{m=0}^{\infty} \exp(-\beta L E_m) \Phi_m(\mathbf{R}) \Phi_m^*(\mathbf{R}'), \quad (28)$$

where

$$\hat{H}\Phi_m(\mathbf{R}) = E_m\Phi_m(\mathbf{R}). \quad (29)$$

The Schrödinger equation with a random potential is a well known problem that has been intensely studied for a long time [16, 17, 18, 19]. The main property that we will use is that when $V(\mathbf{R})$ has short range correlations (i.e. correlation length is shorter than any other length scale in the problem), and if the system size is infinite, then in any dimension all eigenstates with energy below a critical energy E_M (referred to as the mobility edge) are exponentially localized in the form

$$\Phi_m(\mathbf{R}) \sim \exp(-|\mathbf{R} - \mathbf{R}_m|/\ell_m). \quad (30)$$

Here \mathbf{R}_m is the localization center of the m^{th} state, and ℓ_m is the localization length of that state. The localization length satisfies $1/\ell_m = \beta\sqrt{2M|E_m|}$ for $E_m \ll 0$, i.e. deep in the tail region. For $E > E_M$ extended states exist when $d > 2$. For $d = 1, 2$ there is no mobility edge and all states are exponentially localized. The states with energies $E > E_M$ are called extended since they are no longer localized but are spread over a finite fraction of the system. Also, it is known that the eigenvalues of the localized states are discrete, while the eigenvalues of the extended states form a continuum.

For finite system size, or if $\mu \neq 0$ in the Hamiltonian given in Eq. (27), the above discussion has to be modified. First, the eigenfunctions are always discrete in any dimensions. But even in one dimension as the energy increases the width of the localized states eventually becomes comparable to the system size and thus a localized particle of that energy can go from one end of the sample to the other. Thus the distinction between localized and extended states becomes blurred for a finite system at energies much above the ground state. Nevertheless, there will still be a qualitative difference between the low energy tail states and the higher energy states with large localization lengths.

All the physical properties of the polymer chain can be expressed in terms of the eigenstates of Schrödinger equation. For instance we can write the end-to-end distance for a given realization of the random potential as

$$\langle \mathbf{R}_F^2(L) \rangle_V = \frac{2 \sum_m \left(a_m \int d\mathbf{R} \mathbf{R}^2 \Phi_m^*(\mathbf{R}) - \left| \int d\mathbf{R} \mathbf{R} \Phi_m(\mathbf{R}) \right|^2 \right) \exp(-\beta L E_m)}{\sum_m |a_m|^2 \exp(-\beta L E_m)}, \quad (31)$$

where $a_m = \int d\mathbf{R} \Phi_m(\mathbf{R})$, and where $\langle \cdot \rangle_V$ refers to a configurational average for the case of a fixed realization of random potential. When L is large enough so that $(E_1 - E_{gs})L \gg 1$, where E_1 is the eigenvalue of the first excited state and E_{gs} is the ground state eigenvalue, then only the ground state contributes. In this case we have

$$\langle \mathbf{R}_F^2(L) \rangle_V = 2 \frac{\int d\mathbf{R} \mathbf{R}^2 \Phi_{gs}(\mathbf{R})}{\int d\mathbf{R} \Phi_{gs}(\mathbf{R})} - 2 \left(\frac{\int d\mathbf{R} \mathbf{R} \Phi_{gs}(\mathbf{R})}{\int d\mathbf{R} \Phi_{gs}(\mathbf{R})} \right)^2, \quad (32)$$

where $\Phi_{gs}(\mathbf{R})$ is the ground state eigenfunction. It can be shown that the ground state wave function is positive definite and so in the large L limit $\langle \mathbf{R}_F^2(L) \rangle^{1/2}$ can be interpreted as the width of the ground state eigenfunction. Assuming the ground state has the form

given in Eq. (30), we can write $\langle \mathbf{R}_F^2(L) \rangle_V = 2d(d+1)\ell_{gs}^2$, where $\ell_{gs} = \ell_0$ is the localization length of the ground state. Upon averaging over all realizations of the random potential we get that $\overline{\langle \mathbf{R}_F^2(L) \rangle} = 2d(d+1)\overline{\ell_{gs}^2}$, and so the quenched average of the end-to-end distance, in the long chain limit, is proportional to the square of the average localization length of the ground state eigenfunction.

2.4. Localized eigenstates and glassy behavior

Using the path integral mapping we can evaluate the partition sum by solving the discretized Schrödinger equation. In $d = 1$ this can be accomplished by simply diagonalizing an $N \times N$ Hamiltonian matrix, with lattice spacing $\Delta = S/N$, where S is the system size. Details of the numerical procedure are given in [20]. Using the lattice computation, we explore the connection between the eigenstates of the Schrödinger equation and the physical properties of the polymer chain. Here, we focus on the probability distribution defined as

$$P(\mathbf{R}, L) = Z(\mathbf{R}, \mathbf{R}, L) / \int Z(\mathbf{R}, \mathbf{R}, L) d\mathbf{R} \quad (33)$$

which can be interpreted as the probability of finding a closed polymer chain of length L which passes through the point \mathbf{R} (for a given realization of the random potential). We consider this probability distribution since it gives the most direct connection between the chain properties and the eigenfunctions of the Schrödinger equation. In Fig. 1 we plot $P(R, L)$ vs. R for four different chain lengths. We also include a plot of the random potential sample that is used. From the plot we can see clearly that as the chain length is increased the probability distribution tends to localize around a few valleys of the random potential landscape. As L is increased further there is only one peak as the chain finds the most favorable position. These results can be explained in terms of the eigenfunctions of the Schrödinger equation using the expansion

$$Z(\mathbf{R}, \mathbf{R}; L) = \sum_m \exp(-\beta L E_m) |\Phi_m(\mathbf{R})|^2. \quad (34)$$

Which shows that as L is increased the localized tail states dominate the partition sum until only the ground state remains when $(E_1 - E_{gs})L \gg 1$.

The dominance of tail states for long polymer chains leads to large sample-to-sample variations in measured physical quantities. This is because the partition sum, for a given realization of the random potential, is dominated by a few favorable conformations which are strongly sample dependent. In Fig. 2.4 we plot the relative sample-to-sample fluctuations of the end-to-end distance $\langle \mathbf{R}_F^2(L) \rangle$, as a function of chain length. The relative sample-to-sample fluctuation is defined as $\Delta_F / \overline{\langle \mathbf{R}_F^2(L) \rangle}$ with

$$\Delta_F = \left(\overline{\langle \mathbf{R}_F^2(L) \rangle^2} - \overline{\langle \mathbf{R}_F^2(L) \rangle}^2 \right)^{1/2}, \quad (35)$$

and where the averaging is done over many realizations of the random potential. From the plot it is clear that as the length of the chain is increased the sample-to-sample fluctuations increases dramatically at a chain length $L_c \sim 0.5$.

Large sample-to-sample fluctuations in measured physical quantities are typical of glassy systems, which are a broad class of systems characterized by rugged energy landscapes [21]. This is precisely the case here, where the free energy of a long chain will

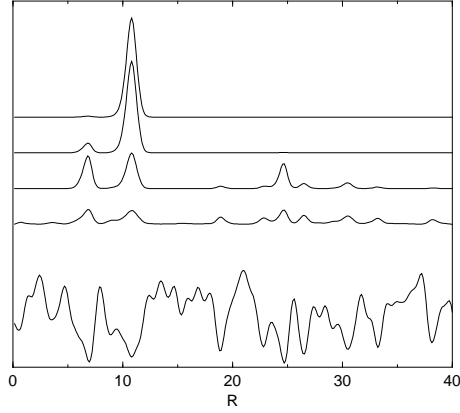


Figure 1. Plot of $P(R, L)$ vs R for four values of L . The bottom most curve is the random potential sample that is used. From bottom to top we use $L = .3, 1, 10, 20$. The model parameters are $M = 1/2$, $g = 25$, $\beta = 1$, and $\mu = 0.01$. We use a lattice of size $S=40$ with $\Delta = 0.2$. The random potential is modeled by generating N numbers $\{V_\xi(i)\}_{i=1,\dots,N}$ which satisfy $\langle V_\xi(i)V_\xi(i+l) \rangle \propto \exp(-\Delta^2 l^2 / \xi^2)$, where $\xi = 1/\sqrt{2}$.

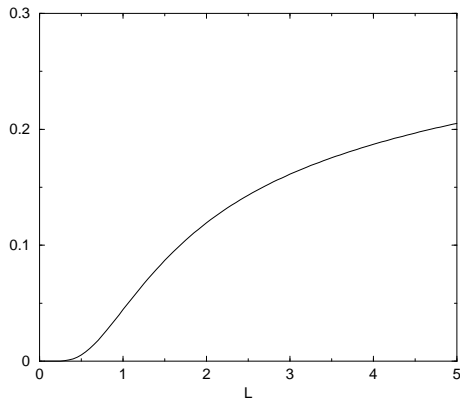


Figure 2. Plot of $\Delta_F / \sqrt{\overline{\mathbf{R}_F^2(L)}}$ vs. L . The parameters are the same as in Fig. 1 and we average over 1000 random potential realizations.

be dominated by conformations that reside in the deep valleys of the random potential landscape. The main new result here is that the emergence of glassy characteristics of a polymer chain in random media can be traced to the dominance of localized tail states of the Schrödinger equation.

2.5. Averaging over disorder: The replica trick

The numerical results in the previous section reveal that a polymer in a random potential can be viewed as a glassy system. In order to develop this point of view, we apply the replica method, which has been successfully applied in the study of glassy systems [21]. The replica approach was invented in order to compute quenched averages such as $\overline{\langle \mathbf{R}_F^2(L) \rangle}$, as given in Eq. (10), which is difficult since it entails averaging a ratio of the partition sum. The starting point is the formal identity

$$\ln(Z) = \lim_{n \rightarrow 0} \frac{Z^n - 1}{n}, \quad (36)$$

which can be used to calculate the quenched free-energy

$$\overline{F} = -kT \overline{\ln(Z)} = -kT \lim_{n \rightarrow 0} \frac{\overline{Z^n} - 1}{n}, \quad (37)$$

where the order of the averaging and taking the $n \rightarrow 0$ limits has been interchanged, hopefully with no ill ramifications. The average of a term like Z^n , where n is a positive integer, is easy to implement by creating n -identical copies of the system, referred to as replicas, and then averaging over the random potential. This process of averaging results in interactions between different replicas. The resulting analytical expression is then continued analytically to $n = 0$.

Introducing n -copies of the system and computing $\overline{Z^n}$ it is straight forward to show that the average end-to-end distance can be formally written as

$$\overline{\langle \mathbf{R}_F^2(L) \rangle} = \lim_{n \rightarrow 0} \frac{\int \prod_{a=1}^n d\mathbf{R}_a \prod_{a=1}^n d\mathbf{R}'_a (\mathbf{R}_1 - \mathbf{R}'_1)^2 Z_n(\{\mathbf{R}_a\}, \{\mathbf{R}'_a\}; L)}{\int \prod_{a=1}^n d\mathbf{R}_a \prod_{a=1}^n d\mathbf{R}'_a Z_n(\{\mathbf{R}_a\}, \{\mathbf{R}'_a\}; L)}, \quad (38)$$

where

$$Z_n(\{\mathbf{R}_a\}, \{\mathbf{R}'_a\}; L) = \int_{\mathbf{R}_a(0)=\mathbf{R}_a}^{\mathbf{R}_a(L)=\mathbf{R}'_a} \prod_{a=1}^n [d\mathbf{R}_a] \exp(-\beta H_n), \quad (39)$$

and where

$$H_n = \frac{1}{2} \int_0^L du \sum_a \left[M \left(\frac{d\mathbf{R}_a(u)}{du} \right)^2 + \mu \mathbf{R}_a^2(u) \right] - \frac{\beta}{2} \int_0^L du \int_0^L du' \sum_{ab} f((\mathbf{R}_a(u) - \mathbf{R}_b(u'))^2). \quad (40)$$

Thus, the averaged equilibrium properties of the polymer can be extracted from an n -body problem by taking the $n \rightarrow 0$ limit at the end. This limit has to be taken with care, by solving the problem analytically for general n , before taking the limit of $n \rightarrow 0$.

2.6. The Replica Variational Approach

In order to compute quenched averages of the polymer chain we will have to solve the n -body replicated partition sum given in Eq. (40). This path integral cannot be evaluated analytically and a variational approach has been used in Refs. [22, 8] to make further progress. The procedure is to follow the work of Feynman [7] and others [23, 24] and model H_n by a solvable trial Hamiltonian h_n which is determined by the stationarity of the variational free energy

$$n\langle F \rangle = \langle H_n - h_n \rangle_{h_n} - \frac{1}{\beta} \ln \int [d\mathbf{R}_1] \cdots [d\mathbf{R}_n] \exp(-\beta h_n). \quad (41)$$

Following [22] we use a quadratic trial Hamiltonian of the form

$$h_n = \frac{1}{2} \int_0^L du \sum_a \left[M \left(\frac{d\mathbf{R}_a(u)}{du} \right)^2 + \mu \mathbf{R}_a^2(u) \right] - \frac{1}{4L} \int_0^L du \int_0^L du' \sum_{ab} p_{ab} (\mathbf{R}_a(u) - \mathbf{R}_b(u'))^2, \quad (42)$$

where the matrix elements p_{ab} are the variational parameters. The physical motivation for this ansatz is that the replica-replica interaction in the original Hamiltonian is modeled by a quadratic interaction which can be different for different replica pairs. Also, the form of the quadratic interaction was chosen specifically [22] to preserve the translational invariance of the original Hamiltonian. Apart from the μ -dependent term, (or alternatively in the limit $\mu \rightarrow 0$), the original Hamiltonian H_n given in Eq. (40) is invariant under the transformation

$$\mathbf{R}_a(u) \rightarrow \mathbf{R}_a(u) + \mathbf{C}, \quad a = 1, \dots, n \quad (43)$$

where \mathbf{C} is a constant vector. This reflects the fact that in the infinite system, without a confining harmonic term, after averaging over the random potential the interaction is translational invariant. A good variational Hamiltonian must be one that can preserve this translational symmetry. Thus the variational ansatz must be rich enough to implement the relation (43). The ansatz chosen by EM [15] violated this translational invariance for any $q \neq 0$, where q denoted their single variational parameter. This imposed an unphysical origin on the system when none existed in the infinite volume limit that they considered. It was actually shown in Ref. [22] that if the variational ansatz is rich enough the translation invariance actually emerges from the variational extremization even if not assumed explicitly for the trial Hamiltonian.

We will now assume that in the $n \rightarrow 0$ limit the matrix p_{ab} can be parameterized according to the 1-step replica symmetry breaking scheme of Parisi [24]. In the 1-step RSB scheme, the matrix p_{ab} can be parameterized as $(\tilde{p}, p(x))$ with

$$p(x) = \begin{cases} p_0 & 0 < x < x_c \\ p_1 & x_c < x < 1 \end{cases}, \quad (44)$$

and where x is Parisi's replica index. See Figure(3) for an illustration.

Calculating the variational free energy using Eq. (41) it could be expressed [22] in the limit $n \rightarrow 0$ as a function of the four variational parameters. i.e. $F = F(\tilde{p}, p_0, p_1, x_c)$.

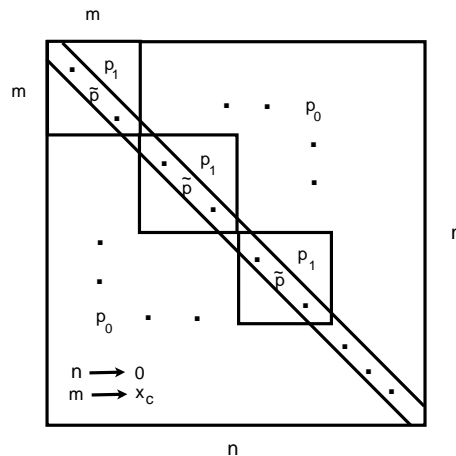


Figure 3. Illustration of first step replica symmetry breaking. The limits $n \rightarrow 0$ and $m \rightarrow x_c$ have to be taken with $0 < x_c < 1$.

The stationarity of the free energy yields four coupled non-linear equations for the four variational parameters. In the limit of small μ (large volume) and long chains (L large) these equations were solved analytically. Denoting by λ the combination

$$\lambda = \mu - \tilde{p} + (1 - x_c)p_1 + x_cp_0, \quad (45)$$

we find from the analytical variational solution

$$\lambda \sim (g |\ln \mu|)^{4/(4-d)}. \quad (46)$$

From this final result we can obtain the radius of gyration which can be shown to be proportional to $\lambda^{-1/4}$. Recalling also that $|\ln \mu| \propto \ln \mathcal{V}$, we find

$$R_g \sim \lambda^{-1/4} \sim (g |\ln \mu|)^{-1/(4-d)} \sim (g \ln \mathcal{V})^{-1/(4-d)}, \quad (47)$$

a result which coincides with the prediction of Cates and Ball for the case of a finite volume. It could also be shown that a replica-symmetric ansatz for the matrix p yields a result consistent with the annealed average of the disorder where the chain collapses in the limit of $L \rightarrow \infty$.

For non-asymptotic values of μ and L the non-linear stationarity equations could be solved numerically [20] using a standard iterative method [25]. We found that for a given set of parameters there is a chain length L_c (which depends on the strength of the disorder) such that for $0 < L < L_c$ there is only a replica symmetric solution. This is the case when the variational parameters satisfy $x_c = 1$ and $s_0 = s_1$. For $L > L_c$ there is still a replica symmetric solution but we also find an additional replica symmetry breaking solution. So in this regime we find an additional solution such that $0 < x_c < 1$ and $s_0 \neq s_1$. In order to decide which solution correctly describes the physics in that regime we compare their respective predictions to the lattice computation of $\overline{\langle \mathbf{R}_F^2(L) \rangle}$.

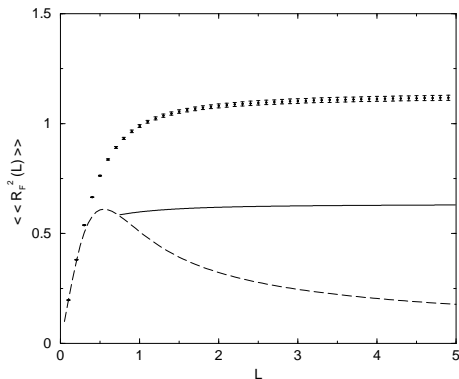


Figure 4. Plot of $\langle \mathbf{R}_F^2(L) \rangle$ vs. L . The dotted line is generated by averaging over 10000 samples, and error bars are found by computing the standard deviation of 10 sets of 1000 samples. The dashed line is the RS solution, and the solid line is the RSB solution.

In Fig. 4 we plot the mean squared displacement $\langle \mathbf{R}_F^2(L) \rangle$ vs. L for a given set of parameters. We plot this quantity using the lattice result, and also using the two predictions of the variational method. Note that in the labels of the plots the average over the disorder is denoted by a second set of brackets rather than an over-bar. For L below $L_c \approx 0.73$ there is only a RS solution which is very close to the lattice prediction. For L greater than L_c the RS and RSB solutions are different and it is clear that the RSB solution is closer to the lattice result. We can see that the end-to-end distance saturates at a constant value as L increases. This behavior is correctly predicted by the RSB solution but not by the RS solution.

So far we have seen that the glassy characteristics of a polymer in a short range correlated random potential is closely related to the dominance of low energy eigenfunctions. We also know that the variational solution possesses a RS solution for $L < L_c$ and an RSB solution for $L > L_c$. It is well known that replica symmetry breaking is typically associated with glassy behavior, and for our model we show that the onset of RSB is precisely when the system begins to exhibit glassy behavior. The variational parameter that best reveals the transition between RS and RSB is the break point x_c . If $x_c = 1$ then there is only an RS solution, and if $0 < x_c < 1$ then that corresponds to an RSB solution. In Fig. 5 we plot x_c vs. L using the same parameters that were used in Fig. 4. We can see that onset of the RSB solution is at $L_c \approx .73$, after which we find that the break point decreases like $x_c \propto 1/L$. If we compare this result to the plot of $\Delta_F / \langle \mathbf{R}_F^2(L) \rangle$ vs L in Fig. 2.4, we see that near $L_c \approx 0.5$ the sample-to-sample fluctuations begin to rise rapidly. This result provides strong evidence that when the RSB solution is valid the polymer chain does indeed exhibit glassy behavior.

2.7. Physical interpretation of the 1-step RSB solution

In this section we study the physical interpretation of the replica symmetry breaking solution. Our purpose is to see if the underlying physical picture predicted by 1-step

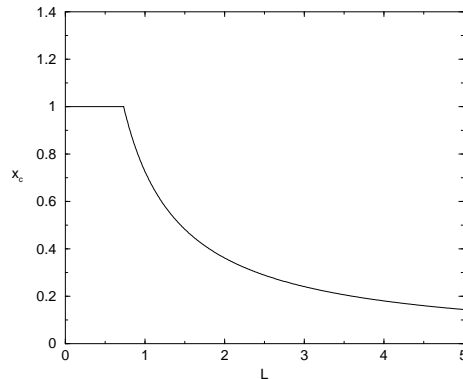


Figure 5. Plot of x_c vs. L . The parameters are the same as those used in Fig. 4.

RSB is indeed consistent with the presence of exponentially localized eigenstates. The following analysis is valid for a very long polymer (large L) when the system becomes glassy. We begin by evaluating the replicated partition sum defined as

$$\tilde{Z}_n(\{\mathbf{R}_a\}) = \int_{\mathbf{R}_a(0)=\mathbf{R}_a}^{\mathbf{R}_a(L)=\mathbf{R}_a} \prod_{a=1}^n [d\mathbf{R}_a] \exp(-\beta h_n), \quad (48)$$

where h_n is the quadratic trial Hamiltonian in Eq. (42). Since h_n is quadratic the path integrals can be evaluated analytically and the final result can be written in the form

$$\tilde{Z}_n(\{\mathbf{R}_a\}) = \text{const.} \times \exp\left(-\frac{1}{2} \sum_{ab} Q_{ab}^{-1} \mathbf{R}_a \cdot \mathbf{R}_b\right). \quad (49)$$

The details of this calculation along with the relationship between the matrices Q_{ab} and p_{ab} are given [20]. Now, since p_{ab} was parameterized according to the 1-step RSB scheme, it implies that Q_{ab} can also be parameterized in the same way.

Mezard and Parisi [24] discuss the interpretation of a representation of the form (49) for the case of directed polymers. In particular they show how to deduce the structure of the probability distribution

$$P_V(\mathbf{R}) = \tilde{Z}_V(\mathbf{R}, L) / \int d\mathbf{R} \tilde{Z}_V(\mathbf{R}, L), \quad (50)$$

which is the probability of finding a polymer loop that passes through \mathbf{R} for a given realization (which we denote by V) of the the random potential. Here $\tilde{Z}_V(\mathbf{R}, L)$ is just the partition sum $Z(\mathbf{R}, \mathbf{R}; L)$ as given in Eq. (5). This probability is related to the replicated partition function given in Eq. (48) by

$$P_V(\mathbf{R}) = \lim_{n \rightarrow 0} \int d\mathbf{R}_2 \cdots d\mathbf{R}_n \tilde{Z}_n(\{\mathbf{R}_a\})_{\mathbf{R}_1=\mathbf{R}}. \quad (51)$$

Mezard and Parisi's analysis has to be adapted for the case of real (non-directed) polymers of length L in a random potential which is independent of time. The changes will be pointed out below.

If Q_{ab} is parameterized by $\{\tilde{q}, q(x)\}$ such that

$$q(x) = \begin{cases} q_0 & x < x_c \\ q_1 & x > x_c \end{cases}, \quad (52)$$

one proceeds to obtain $P_V(\mathbf{R})$ by the following procedure:

1. For each sample (a realization of the random potential) generate a random variable \mathbf{R}_0 which is picked from the distribution

$$\mathcal{P}(\mathbf{R}_0) = \frac{1}{(2\pi q_0)^{d/2}} \exp\left(-\frac{\mathbf{R}_0^2}{2q_0}\right). \quad (53)$$

2. Consider a set of "states" labeled by the index α whose physical meaning will be elucidated shortly. Each of these states is characterized by a weight W_α and a position variable \mathbf{R}_α . Given \mathbf{R}_0 , the variables \mathbf{R}_α are an infinite set of uncorrelated random variables distributed according to

$$\mathcal{P}(\mathbf{R}_1, \mathbf{R}_2, \dots) = \prod_\alpha \frac{1}{(2\pi(q_1 - q_0))^{d/2}} \exp\left(-\frac{(\mathbf{R}_\alpha - \mathbf{R}_0)^2}{2(q_1 - q_0)}\right). \quad (54)$$

The distribution of weights will be discussed below.

3. Given these "states" for a given sample, The probability distribution $P_V(\mathbf{R})$ for that sample has the form

$$P_V(\mathbf{R}) = \sum_\alpha W_\alpha \frac{1}{(2\pi(\tilde{q} - q_1))^{d/2}} \exp\left(-\frac{(\mathbf{R} - \mathbf{R}_\alpha)^2}{2(\tilde{q} - q_1)}\right). \quad (55)$$

The weights W_α are given in terms of some "free energy" variables f_α :

$$W_\alpha = \frac{\exp(-\beta f_\alpha)}{\sum_\gamma \exp(-\beta f_\gamma)}. \quad (56)$$

These free energy variables are chosen from an exponential distribution

$$P[f_\alpha] \propto \exp(x_c \beta f_\alpha) \theta(f - \bar{f}), \quad (57)$$

where \bar{f} is an upper cutoff.

What is the meaning of these variables in the present case? To determine the weights W_α we compare Eq. (55) to the eigenfunction expansion given in Eq. (34). From Eq. (34) together with Eq. (50) it becomes clear that

$$P_V(\mathbf{R}) = \sum_\alpha A_\alpha |\Phi_\alpha(\mathbf{R})|^2, \quad (58)$$

where

$$A_\alpha = \frac{\exp(-\beta L E_\alpha)}{\sum_\gamma \exp(-\beta L E_\gamma)}. \quad (59)$$

Comparing Eq. (55) and Eq. (59) it becomes obvious that $W_\alpha = A_\alpha$ and

$$\Phi_\alpha^2(\mathbf{R}) \propto \exp\left(-\frac{(\mathbf{R} - \mathbf{R}_\alpha)^2}{2(\tilde{q} - q_1)}\right). \quad (60)$$

Hence, the “states” labeled by α are in our case the actual eigenstates of the imaginary time Schrödinger equation. These are localized tail states centered at position \mathbf{R}_α with an associated “weight” W_α . Thus the 1-step RSB solution approximates the tail states by a fixed Gaussian form.

The width of these Gaussians, denoted by w_0 , give an estimate of the size of the polymer chain i.e. $w_0 \sim R_F$. In the limit of large L and small μ it can be shown to leading order [22] that $w_0^2 \sim d/(2\beta\sqrt{\lambda M})$, where

$$\lambda = \frac{d^{4/(4-d)}}{(2\pi)^{2d/(4-d)}} (\beta^2 M)^{(4+d)/(4-d)} (g |\ln \mu|)^{4/(4-d)}. \quad (61)$$

So in terms of the disorder strength and the system size the chain size scales like

$$R_F \propto (g |\ln \mu|)^{-1/(4-d)} \propto (g \ln \mathcal{V})^{-1/(4-d)}. \quad (62)$$

It should be emphasized that the subtle dependence on the volume of the system is a direct consequence of replica symmetry breaking. In fact, as shown in Fig. 4 the replica symmetric solution does not correctly describe the size of the polymer chain, since it fails to capture the dominance of localized tail states.

We now consider the distribution $P(\mathbf{R}_\alpha)$ given in Eq. (54). This is just the distribution for the localization centers \mathbf{R}_α for a given value of \mathbf{R}_0 . Hence, we can calculate the average distance between the localized states for a given sample. We find that the width w of the Gaussian $P(\mathbf{R}_\alpha)$ satisfies $w^2 = d(q_1 - q_0)$. For small μ and large L it is straight forward to show that that $w^2 \approx d/(\beta\mu L x_c)$, where the break point x_c is given by

$$x_c = \frac{1}{L} \left(\frac{d^{d-2}}{(2\pi)^d} g^2 \beta^{d+4} M^d |\ln \mu|^{d-2} \right)^{-1/(4-d)}. \quad (63)$$

2.8. Density of states and the 1-step RSB solution

To develop the analogy further we first notice that the free energies f_α are equal to LE_α . This make sense if we think of $|E_\alpha|$ as representing the binding energy per monomer, and thus $f_\alpha = LE_\alpha$ represent the total energy of the chain. These arguments lead us to expect that within the 1-step RSB scheme, the energy variables E_α are independent random variables taken from an exponential distribution:

$$P[E_\alpha] \propto e^{\beta L x_c E_\alpha} \theta(\bar{E} - E_\alpha), \quad (64)$$

with \bar{E} being some energy scale determined by the upper cutoff of the tail region. We will now argue that the distribution given above is just the expected distribution of ground-state energies i.e. the probability of finding the lowest energy level to have energy E . We first review some very basic results of extreme value statistics as presented in Ref. [26]. Given K independent and identically distributed random variables E_i , pulled from a distribution of the form

$$\tilde{P}(E) = \frac{A}{|E|^\alpha} \exp(-B|E|^\delta), \quad (65)$$

the probability that the lowest of the K energies is E (for $E \rightarrow -\infty$ and $K \rightarrow \infty$) is given by

$$P(E) \propto \exp [B\delta |E_c|^{\delta-1} E] , \quad (66)$$

where

$$E_c = - \left(\frac{\log(K)}{B} \right)^{1/\delta} . \quad (67)$$

The value of E_c , the lowest energy expected to be attained in K trials, is easily obtained from

$$\int_{-\infty}^{E_c} dE \tilde{P}(E) \simeq 1/K . \quad (68)$$

The reason why we chose a distribution of the form given in Eq. (65) is that in $d = 1$ the probability $\tilde{P}(E)$ is known to have that form exactly for the case of delta correlated random potentials (see [27]). For $d > 1$ Lifshits [19] argued that the form given by Eq. (65) is also valid. Our goal now is to see if the distribution Eq. (64) derived using the 1-step RSB solution is indeed consistent with the distribution Eq. (66) predicted using extreme value statistics.

Comparing Eq. (64) and Eq. (66) we find that for consistency the break point should satisfy

$$x_c = \frac{\delta}{\beta L} B^{1/\delta} (\log(K))^{(\delta-1)/\delta} . \quad (69)$$

Notice that the $1/L$ behavior of x_c is exactly the same as was found analytically for large L in Ref. [22] and numerically for any $L > L_c$ in the present work. We can go further by using the fact that the number of energy levels K , within a fixed energy interval is directly proportional to the system size, which in our formulation is effectively determined by μ . Assuming $\log(K) \propto |\log(\mu)|$ and comparing to the approximate solution for x_c in Eq. (63) we find that $\delta = (4 - d)/2$ and $B \propto 1/g$. Now $\tilde{P}(E)$ is just proportional to the density of states $\rho(E)$, and it is known exactly in one dimension. Indeed, when $d = 1$, $\delta = 3/2$ and $B \propto 1/g$. For $2 \leq d < 4$, δ agrees with the result derived by Lifshits [19]. Hence, the exponent δ and the disorder dependence of B is correctly predicted by the 1-step RSB solution.

The above results show that the 1-step RSB solution correctly predicts some important features of the eigenvalue distribution. More importantly, we have shown that the 1-step RSB solution can be interpreted in terms of the eigenstates of the Schrödinger equation with a random potential. However, there are differences and these reveal the limitations of the 1-step RSB solution. For example, all the localized states are approximated by the same Gaussian profile when in fact the localization lengths should increase with energy.

3. Localization of polymers in a medium with fixed random obstacles

In this section we discuss the static properties of a Gaussian polymer chain without excluded volume interactions that is confined to a medium populated with quenched

random obstacles. It is important to distinguish between the following two important cases that have been discussed in the literature:

1. A Gaussian random potential with short range correlations.
2. Random obstacles which prevent the chain from visiting certain sites.

Numerical simulations performed in three dimensions were restricted, to our knowledge, only to the case of random obstacles [28, 29, 30]. On the other hand, extensive analytical work using the replica variational approach and Flory type free energy arguments, has been done for the case of a Gaussian random potential [13, 15, 20, 22, 11]. The case of a bounded (saturated) random potential was also addressed in Ref. [13]. It was not clear to us to what extent these theoretical investigations could be applied to the case of infinitely strong random obstacles placed randomly in the medium, as simulated numerically. This motivated us to investigate this problem in detail [31]. The results indicated that only in a special case (a small value of the embedding volume) the two problems mentioned above are similar, but otherwise they are quite different.

We will assume that the obstacles are infinitely strong—they totally exclude the chain from visiting a given site occupied by an obstacle. Each obstacle is taken to be a block of volume a^d , where d is the number of spatial dimensions and where a is the linear dimension of the block. We take for simplicity the polymer bond length b to be approximately equal to a . Thus, a will be the small length scale in the problem, and we will measure all distances in units of a . The obstacles are placed on the sites of a cubic lattice with lattice spacing a . We denote by x the probability that any given lattice site is occupied by an obstacle (block). Our main results will concern the case of small x , in particular $x < x_c$, where x_c refers to the percolation threshold ($x_c = 0.3116$ for a cubic lattice in $d = 3$), but we will also comment on the case of a larger concentration of obstacles. We denote by \mathcal{V} the total volume of the system.

Assume that the chain is occupying a spherical region (lacuna) of volume $\Omega \sim R^d$. In this region the actual volume fraction of obstacles will be denoted by \hat{x} . It is crucial to realize that although the average number of obstacles per site is fixed by x , the actual number of obstacle in a small region of volume $\sim R^d$ is a fluctuating quantity which occurs with probability $b(R^d \hat{x}; R^d, x)$, where

$$b(k; n, p) = \binom{n}{k} p^k (1-p)^{n-k}, \quad (70)$$

denotes the binomial probability distribution.

In the limit where the system has infinite volume \mathcal{V} the free energy for the chain is given by

$$F(R, \hat{x}) = -L \ln(z) + \frac{L}{R^2} + L\hat{x} - \ln[b(R^d \hat{x}; R^d, x)], \quad (71)$$

All these terms originate from entropy $F = -TS$ where for simplicity we take $T = 1$ since the temperature does not play a significant role here with respect to the results. The first term originates from the entropy of a free chain in d -dimensions where z is the coordination number which for a cubic lattice is equal to $2d$. The second term originates from the entropy of confinement in a cavity of radius R . The third term is the entropy loss due to obstacles. This linear dependence is justified in Ref. [31] and in the Appendix

therein. The fourth term represents an entropy given by the logarithm of the probability to have a region of size Ω with $\Omega\hat{x}$ obstacles. This free energy, valid for $\mathcal{V} \rightarrow \infty$, is called the annealed free energy since when the polymer can sample the entire space it is the same as the random potential adjusting itself to the polymer configuration. The free energy has to be minimized (the entropy maximized) with respect to R and \hat{x} . The most favorable value of \hat{x} is 0. Since $b(0; R^d, x) = (1-x)^{R^d}$, we find

$$F(R) = -L \ln(z) + \frac{L}{R^2} - R^d \ln(1-x). \quad (72)$$

This free energy has now to be minimized with respect to R to yield

$$R_{m,annealed} \sim \left(\frac{L}{|\ln(1-x)|} \right)^{1/(d+2)}. \quad (73)$$

Thus the size of the chain grows with L , but with an exponent smaller than 1/2, the free chain exponent.

So far we discussed the case of an infinite volume \mathcal{V} . In a finite volume we find that the so called quenched and annealed case differ, at least when the volume is not too big. We actually find that there are three regions as a function of the size of the system volume \mathcal{V} . First, if $\mathcal{V} < \mathcal{V}_1 \simeq \exp(x^{-(d-2)/2}/(1-x))$, it is unlikely for a chain of volume $\Omega \sim R^d$ to find a region which is totally free of obstacles. Thus \hat{x} does not vanish in this regime. To proceed further we must use an approximation to the binomial distribution $b(\Omega\hat{x}; \Omega, x)$.

If Ω is not too small we can approximate the binomial distribution by a normal distribution [32]

$$b(\Omega\hat{x}; \Omega, x) \approx (2\pi\Omega x(1-x))^{-1/2} \exp\left(-\frac{\Omega(\hat{x}-x)^2}{2x(1-x)}\right). \quad (74)$$

This approximation is good provided $\Omega x \gg 1$ and $\Omega(1-x) \gg 1$. We verified that these conditions are indeed met in our case when x is small.

In a finite volume \mathcal{V} , the lowest expected value of \hat{x} , to be denoted by \hat{x}_m , can be found from the tail of the distribution

$$\int_0^{\hat{x}_m} d\hat{x} \exp\left(-\frac{\Omega(\hat{x}-x)^2}{2xy}\right) \simeq \frac{\Omega}{\mathcal{V}}, \quad (75)$$

which gives

$$\hat{x}_m \simeq x - \sqrt{\frac{xy \ln \mathcal{V}}{R^d}}, \quad (76)$$

where we put $y \equiv 1-x$. The free energy becomes

$$F_I(R) = -L \ln(z) + \frac{L}{R^2} + Lx - L\sqrt{\frac{xy \ln \mathcal{V}}{R^d}}. \quad (77)$$

The last term in the annealed free-energy is missing since it is negligible for large L when R is independent of L . Minimizing $F(R)$ with respect to R we find

$$R_{mI} \sim (xy \ln \mathcal{V})^{-1/(4-d)} \quad (78)$$

and

$$\hat{x}_{mI} = x - (xy \ln \mathcal{V})^{2/(4-d)}. \quad (79)$$

The result for the radius of gyration of the chain, as represented by R_{mI} is the same result as for the case of the Gaussian distributed random potential, but with the strength g replaced by $x(1-x)$. The polymer in this case is localized and its size is independent of L for large L .

As \mathcal{V} grows R_m decreases until eventually \hat{x}_m vanishes. This happens when $\mathcal{V} = \mathcal{V}_1 \simeq \exp(x^{-(d-2)/2}y^{-1})$. For $\mathcal{V} > \mathcal{V}_1$, R_m is no longer given by R_{mI} , but rather by the solution of $\hat{x}_{mII} = 0$. It is the largest region free of obstacles expected to be found in a volume \mathcal{V} . Rather than using the normal approximation we can estimate R_m directly from the relation

$$(1-x)^\Omega \simeq \Omega/\mathcal{V}, \quad (80)$$

with $\Omega \sim R_m^d$. Solving for R_m we obtain

$$R_{mII} \sim \left(\frac{\ln \mathcal{V}}{|\ln(1-x)|} \right)^{1/d}. \quad (81)$$

The polymer is still localized but the dependence on x and on $\ln \mathcal{V}$ has changed. In this region which we call region II the free energy is given by

$$F_{II} = -L \ln(z) + \alpha L \left(\frac{\ln \mathcal{V}}{|\ln(1-x)|} \right)^{-2/d}, \quad (82)$$

where some undetermined constant α is introduced for later convenience.

As \mathcal{V} grows in region II, R_{mII} continues to grow until it reaches the annealed value given above. This happens when

$$\mathcal{V} = \mathcal{V}_2 \sim \exp(x^{2/(d+2)}L^{d/(d+2)}) \quad (83)$$

to leading order in x , which is enormous for large L . For $\mathcal{V} > \mathcal{V}_2$ we have the third region in which $R_{mIII} = R_{m,annealed}$ and it grows like $L^{1/(d+2)}$.

We can thus summarize the behavior of the end-to-end distance as the function of the system's volume as follows:

$$\text{Region I} \quad \mathcal{V} < \mathcal{V}_1 \simeq \exp(x^{-(d-2)/2})$$

$$R_{mI} \sim (x \ln \mathcal{V})^{-1/(4-d)} \quad (84)$$

$$\text{Region II} \quad \mathcal{V}_1 < \mathcal{V} < \mathcal{V}_2 \sim \exp(x^{2/(d+2)}L^{d/(d+2)})$$

$$R_{mII} \sim \left(\frac{\ln \mathcal{V}}{|\ln(1-x)|} \right)^{1/d}. \quad (85)$$

$$\text{region III} \quad \mathcal{V}_2 < \mathcal{V}$$

$$R_m \sim \left(\frac{L}{|\ln(1-x)|} \right)^{1/(d+2)}. \quad (86)$$

The behavior in region II can be deduced from known results of the density of states for a quantum particle in the presence of obstacles (repulsive impurities). In that case [19] the density of states is given by (when the obstacles are placed on a lattice)

$$\rho(E) \sim \exp(-c|\ln(1-x)|E^{-d/2}), \quad E > 0 \quad (87)$$

with c being some dimension dependent constant and x is the density of impurities. Note that $\rho(E)$ vanishes for $E < 0$. We can estimate the lowest energy in a finite volume \mathcal{V} from the integral

$$\int_0^{E_c} dE \rho(E) \simeq 1/\mathcal{V}, \quad (88)$$

and find

$$E_c \sim \left(\frac{\ln \mathcal{V}}{|\ln(1-x)|} \right)^{-2/d}, \quad (89)$$

and thus the localization length is given by

$$\ell_c \sim |E_c|^{-1/2} \sim \left(\frac{\ln \mathcal{V}}{|\ln(1-x)|} \right)^{1/d}. \quad (90)$$

We now make some remarks on the validity of the spherical droplet approximation. The shape of a long polymer chain is determined by the regions of the random medium that have a lower than average number of obstacles. For $\mathcal{V} > \mathcal{V}_1$ these regions are essentially free of obstacles. The probability of finding such empty regions depends only on its volume and not its shape. However given regions of varying shapes and equal volumes, it will be entropically more favorable for a long polymer chain to reside in a region whose shape is closest to a sphere. This is because the confinement entropy is maximized for a sphere over other shapes of the same volume. The argument is equivalent to that proposed by Lifshits [19] in the context of electron localization and is shown rigorously by Luttinger [33]. For $\mathcal{V} < \mathcal{V}_1$ the relevant regions contain a small number of obstacles but we believe that the same argument should roughly hold and deviations from a spherical shape will be small or irrelevant.

We have compared our analytical results with numerical simulations performed by Dayantis *et al.* [30], and also comment on the relation to earlier simulations done by Baumgartner and Muthukumar [28]. Dayantis *et al.* carried out simulations of free chains (random-flight walks) confined to cubes of various linear dimensions 6 – 20, in units of the lattice constant. These chains can intersect freely and lie on a cubic lattice. They introduced random obstacles with concentrations $x = 0, 0.1, 0.2$ and 0.3 . The length of the chains vary between 18 – 98 steps. They also simulated self-avoiding chains that we will not discuss here. They measured the quenched entropy, the end-to-end distance, and also the radius of gyration which is a closely related quantity. Unfortunately, these

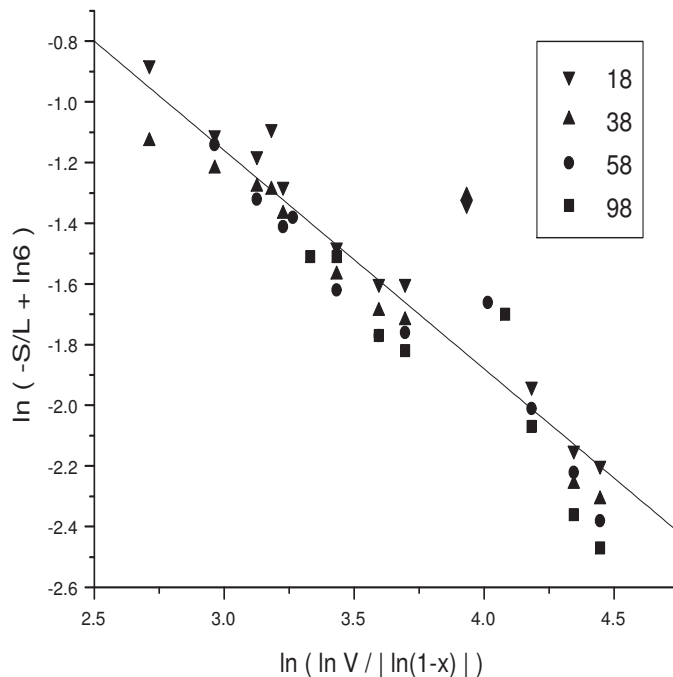


Figure 6. A plot of $\ln(-S/L + \ln 6)$ vs. $\ln(\ln \mathcal{V}/|\ln(1-x)|)$. The labels are marked according to the chain length.

authors did not have a theoretical framework to analyze their data, and thus could not make it collapse in any meaningful way. We show below how it is possible to fit the data nicely to our analytical results.

Even for $x = 0.1$, the value that we get for \mathcal{V}_1 is about 33 which is an order of magnitude smaller than the the smallest volume used in their simulation, which is 216 for a cube of side 6. Hence we expect to be in region II. To check the agreement with our analytical results we show in Figure 6 a plot of $\ln(-S/L + \ln 6)$ vs. $\ln(\ln \mathcal{V}/|\ln(1-x)|)$ where S is the entropy measured in the simulations and $\mathcal{V} = B^3$ for a box of side B . Recall that $F = -S$ and Eq. (82) predicts a straight line with slope $-2/3$. The best fit is obtained for a slope of -0.72 ± 0.05 , which is in excellent agreement with our analytical results in region II.

In order to analyze the simulation results for the end-to-end distance and radius of gyration we have to introduce some additional compensation for the results obtained in the previous section. First we must realize that Eq. (81) is valid only when the number of steps (monomers) is very large. In the simulations they used chains of varying lengths whose size did not yet reach asymptotia. Hence, we introduce a correction factor

$$R_m(L) = R_m(1 - \exp(-L/R_m^2))^{1/2} \equiv R_m f_1(\sqrt{L}/R_m), \quad (91)$$

which interpolates between the size of a free chain as $L \rightarrow 0$ and the value of R_m from Eq. (81) as $L \rightarrow \infty$.

The second correction we have to implement arises when the expected value of the chain is not much smaller than the size of the confining box. Even for a free chain confined to

a box of side B with no obstacles present, the end-to-end distance is not simply $R = L^{1/2}$ for $L^{1/2} < B$ and $R = B$ for larger L . We have to take into account the fact that the length of the chain has a Gaussian distribution about its expected value, and the tail of the Gaussian is cut off by the presence of the box (this is for the absorbing boundary conditions that is used in the simulations). Thus, for the case of no obstacles ($x = 0$), The measured end-to-end distance should approximately be

$$R_c^2 = \int_{-B}^B dR R^2 \exp(-\frac{R^2}{2L}) / \int_{-B}^B dR \exp(-\frac{R^2}{2L}), \quad (92)$$

which gives $R_c = \sqrt{L} f_2(B/\sqrt{L})$ with

$$f_2(x) = \left(1 - \sqrt{\frac{2}{\pi}} \frac{x}{\operatorname{erf}(x/\sqrt{2})} \exp(-x^2/2) \right)^{1/2}. \quad (93)$$

This indeed gives good agreement with the measured values in the no obstacle case. For the obstacle case we thus have to introduce these two corrections in subsequent order:

$$R_{m,corrected} = R_m f_1(\sqrt{L}/R_m) f_2 \left(\frac{B}{R_m f_1(\sqrt{L}/R_m)} \right), \quad (94)$$

where $R_m = R_{mII}$ as given by Eq. (81). (A constant of proportionality of 1.8 has been introduced on the rhs of Eq. (81) to obtain a good fit). In Figure 7 we show a comparison of the simulation results for the end-to-end distance with the calculated results as given by Eq. (81) and Eq. (94). The agreement seems remarkable, since all the data collapses to a straight line with a slope close to 1.

Dayantis *et al.* emphasize that they did not consider concentrations of obstacles above the percolation threshold, which is at $x_c = 0.3116$ for a simple cubic lattice. The reason is that above the percolation threshold the medium of random obstacles begins to form disconnected islands free of obstacles. Thus, in their simulation the polymer chain will only sample a limited fraction of the volume available. What happens is that effectively the volume available for the chain is not the total volume of the cube but rather the volume of the disconnected region it occupies. For most realizations of the random medium this effective volume will be smaller than the value \mathcal{V}_1 , which is the limit of region I of the last section. In that case one expects the end-to-end distance to scale like x^{-1} as given in Eq. (78) instead of like $x^{-1/3}$ as given by Eq. (81). Baumgartner and Muthukumar's simulation was for both below the percolation threshold and also above it ($x = 0.4$ and 0.5). However, they only estimate the exponent above the percolation threshold, and find it to be about -1 . They do not estimate the exponent for x below the percolation threshold, which appears from their data to scale with a much smaller exponent. Thus, it seems likely that the reason these authors report a behavior corresponding to region I, even though their box is quite large, is because the effective volume is small for the cases for which they exceed the percolation threshold.

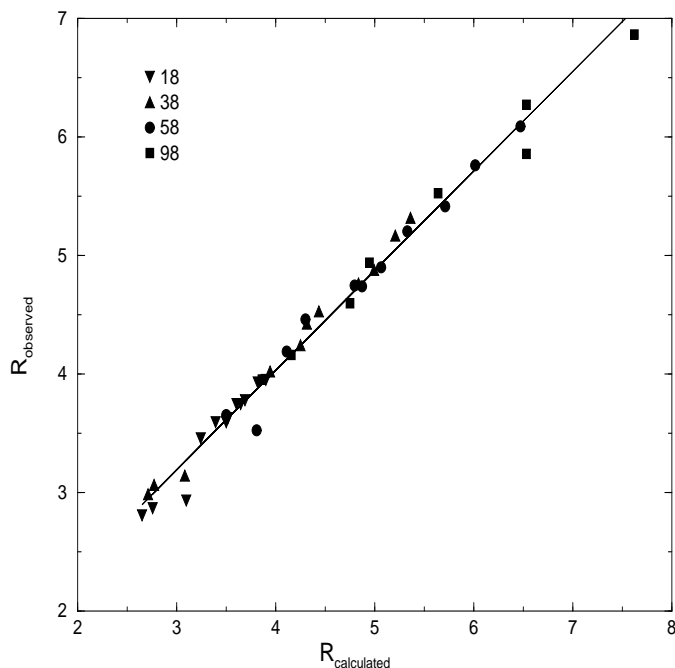


Figure 7. A plot of the observed vs. calculated end-to-end distance

4. Localization and delocalization of polymers with self-avoiding interaction in the presence of disorder

In the previous sections an ideal (Gaussian) chain has been used, which corresponds approximately to the experimental situation at the so called Θ -temperature when the solvent effectively screens the self-avoiding interaction of the chain. In some early papers [28, 11, 34] there was an attempt to include the effects of the self-avoiding interaction of the polymer. These attempts were far from complete. For example in Ref. [11] it was assumed that the conformation of the polymer consists of one spherical blob and it was argued that a quenched random potential is irrelevant for a very long chain when a self-avoiding interaction is present. In Ref. [34] analytical results were obtained for annealed disorder, and simulations were performed for strictly self-avoiding walks. Ref. [28] presents numerical evidence for a size transition of the polymer as a function of the relative strength of the disorder and the self-avoiding interaction. The simulations were carried out for a random distribution of hard obstacles with a concentration exceeding the percolation threshold. In a recent paper [35] we tried to shed more light on this important problem. We have made use mainly of Flory-type arguments, and considered both the case of a Gaussian random potential and the case of randomly placed obstacles. Note that a polymer with self-avoiding interactions cannot be mapped into a quantum particle at a finite temperature in a simple manner, because for a quantum particle there is no impediment to return at a later time (or Trotter time) to a position it visited previously.

An important point to keep in mind is the strength of the excluded volume interaction. If one considers a strictly self-avoiding walk on a lattice (SAW) corresponding to a non-

self-intersecting chain, then the strength of the Edwards parameter v [6] is fixed at $O(1) \times a^3$ where a is the step size (or monomer size) and depends only on the type of lattice. On the other hand one can consider a Domb-Joyce model [36] where there is a finite penalty for self overlapping of polymer segments, and then the strength of v can be varied substantially and reduced continuously to zero. The interplay between the strength of the self-avoiding interaction and the strength of the disorder can then be investigated to a larger extent. Experimentally the Edwards parameter is given approximately [14] by $v = a^3(1 - 2\chi)$, where χ is the Flory interaction parameter, which depends on the chemical properties of the polymer and the solvent, and on the temperature (and pressure). It takes the value $1/2$ at the Θ -point. The case $\chi = 0$ corresponds to a solvent that is very similar to the monomer. In general good solvents have low χ whereas poor solvents have high χ resulting in v being negative. In the following we will restrict ourselves to the case of positive v , which leads to the more interesting and non-trivial results.

We now revisit the meaning of the term localization as applied to polymers in a random medium. Although some authors connect the compact size of the chain when $L \rightarrow \infty$ with the notion of localization, this is actually not so. The compact size should be viewed as a separate feature from the notion of localization. Recall that for a Gaussian chain in an uncorrelated Gaussian random potential of variance g the chain has typical size

$$R_F \propto (g \ln \mathcal{V})^{-1/(4-d)}, \quad (95)$$

and the binding energy per monomer is given approximately by

$$U_{bind}/L \sim -(g \ln \mathcal{V})^{2/(4-d)}. \quad (96)$$

To insure localization, the binding energy of a chain U_{bind} has to exceed the translational entropy $\ln \mathcal{V}$. From Eq. (96) this amounts to the condition

$$\ln \mathcal{V} < L(g \ln \mathcal{V})^{2/(4-d)}, \quad (97)$$

which holds for any $2 \leq d < 4$ when L is large enough (for $2 < d < 4$ and any fixed L , the condition can be satisfied for large enough \mathcal{V}). This condition assures that the polymer will stay confined at a given location and will not, under a some small perturbation move to a different location. Thus repeating an experiment or a simulation with the same fixed realization of the disorder, but with different initial conditions, will result in finding the polymer situated at the same region of the sample as in a previous experiment, provided of course one waits enough time (which can be enormous) for the system to reach equilibrium. We observe that this condition is satisfied for large enough L provided the binding energy per monomer is positive. Another interpretation of the inequality given above in the context of equilibrium statistical mechanics is that the partition sum is dominated by the term involving the ground state as opposed to the contribution of the multitude of positive energy extended states. The contribution of these states is proportional to the volume of the system and thus the inequality above results from the condition

$$\exp(-LE_0) > \mathcal{V}. \quad (98)$$

What we will see in the following sections is that in the presence of a self-avoiding interaction, a localization-delocalization transition occurs when varying the strength of the the self-avoiding interaction for a fixed amount of disorder or alternatively upon varying the strength of the disorder for a fixed value of the self-avoiding interaction.

4.1. A self avoiding chain in a random potential

Consider first the case of a random potential with a Gaussian distribution. For simplicity, the discussion in the rest of this section be limited to three spatial dimensions ($d = 3$). Recall that in the case when there is no self-avoiding interactions the optimal size of a chain R_m is found by minimizing the free energy F in Eq. 23. This yields

$$R_m \sim \frac{1}{g \log(\mathcal{V})} \equiv \frac{1}{G(\mathcal{V})}, \quad (99)$$

where we defined the volume dependent disorder strength by $G(\mathcal{V}) = g \ln(\mathcal{V})$. Substituting this result in F we obtain

$$F_m = -\frac{L}{3R_m^2} \approx -G(\mathcal{V})^2 L. \quad (100)$$

We see that $-F_m/L$ is the binding energy per monomer, and it is strictly positive, so the polymer is localized. In what follows we will assume that g is small enough so that $G \ll 1$ for the given system volume, hence $R_m \gg 1$, and the chain is not totally collapsed unless $\mathcal{V} \rightarrow \infty$.

We now add a self avoiding interaction and assume first that it is small, i.e. $v \ll g$, or at least $v < g$. If the chain is still localized in the same well, which we will see momentarily not to hold when L is large, then

$$F = \frac{L}{R_m^2} - L \sqrt{\frac{g \log(\mathcal{V})}{R_m^3}} + \frac{vL^2}{R_m^3} \approx -G(\mathcal{V})^2 L + vG(\mathcal{V})^3 L^2. \quad (101)$$

Here, besides assuming that v is small we assume for the moment that L is not too big so the last term in the free energy, resulting from the self-avoiding interaction, is small enough so one does not have to take into account the change in R_m due to the presence of v . If we plot F vs. L , we see that it is lowest when

$$L = L_m = \frac{1}{2vG(\mathcal{V})}. \quad (102)$$

Thus if $vg \ll 1$, we have $L_m \gg 1$, and

$$F_m = -\frac{G(\mathcal{V})}{4v}. \quad (103)$$

For $L = 2L_m$ the free energy vanishes and for larger L it eventually increases fast like L^2 . We can now verify that if L does not exceed L_m then the approximation used above, assuming that R_m does not change appreciably from its ideal chain value, is justified. If we differentiate the above F in Eq. (101) with respect to R_m we find

$$R_m \sim \frac{1}{G(\mathcal{V})} \left(1 + \frac{vL}{R_m}\right)^2 \approx \frac{1}{G(\mathcal{V})} (1 + vG(\mathcal{V})L)^2, \quad (104)$$

again omitting constants of order unity. Thus the correction vGL evaluated at $L = L_m$ is of order unity, and we can still use the value $R_m \sim 1/G$.

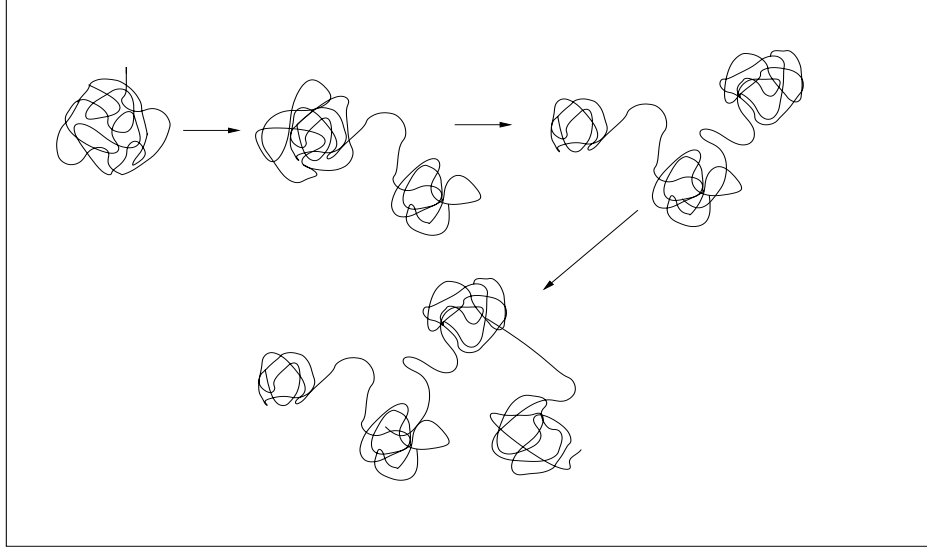


Figure 8. Conformation of a chain consisting of many “blobs” with connecting segments as L increases. Initially the first blob “overflows” and there is “hopping” to another deep minimum. There is a competition between the length of the connecting segment and the probability to find a deep minimum nearby.

For larger L the approximation seems to break down, but fortunately what happens is that since the free energy increases when L exceeds L_m , it is energetically favorable for part of the chain to jump into a distant well. Even though there is a cost for the polymer segment between the wells one still gains in the overall free energy from the binding energy in the wells. Thus the picture that emerges is that as L increases, the chain divides itself into separate blobs with connecting segments. In each blob the number of monomer does not exceed L_m , which is the optimal value for that well. The idea is depicted in Figure 8.

To be more specific we will now construct a model for the free energy of the chain. The first blob will be located in the deepest minimum in the total volume, whose depth is roughly given by $-G(\mathcal{V})^2$ per monomer, where \mathcal{V} is the total volume of the system. Subsequent blobs will reside in the most favorable well within a range Y , which has to be taken self-consistently as the length of the jump. Thus within a range Y the chain is likely to find a potential minimum of depth $-G(Y^3)^2$. The farther you jump, the deeper well you are likely to find. Thus assuming for simplicity that the jumps are roughly of equal size, and there are K blobs in addition to the initial blob, the free energy of the chain will be given roughly by

$$F(w, m, Y; L) \approx -\frac{G(\mathcal{V})}{4v} + K \left(\frac{Y^2}{m} + \frac{m}{Y^2} + \frac{vm^2}{Y^3} - wG(Y^3)^2 + vw^2G(Y^3)^3 \right), \quad (105)$$

with

$$K = \frac{L - L_0}{w + m}, \quad L_0 = \frac{1}{2vG(\mathcal{V})}, \quad G(Y^3) = 3g \ln(Y). \quad (106)$$

We defined w to be the number of monomers in each blob, and m to be the number of monomers in each connecting segment. The term Y^2/m results from the “stretching” entropy of the segment and m/Y^2 from the confinement entropy. The term vm^2/Y^3 represents the self-avoiding interaction for the connecting segments. L_0 is the number of monomers in the initial blob whose free energy was taken care of separately. It is evident that when L is very large we can neglect the free energy of the first blob and also take $K \approx L/(w + m)$. Thus we find for the free energy per monomer

$$f(w, m, Y) \equiv \frac{F(w, m, Y; L)}{L} \approx \frac{1}{w + m} \left(\frac{Y^2}{m} + \frac{m}{Y^2} + \frac{vm^2}{Y^3} - wG(Y^3)^2 + vw^2G(Y^3)^3 \right). \quad (107)$$

This function has to be minimized with respect to w , m and Y to find the parameters giving rise to its lowest value. For the connecting pieces of the chain we did not include a contribution from the random potential since it is expected to average out to zero for these parts. To gain some feeling into the behavior of this function and the values of the parameters which minimize it, we display in Table I the value of the parameters and free energy per monomer for $g = 0.05$ and various values of v , as obtained from a minimization procedure. The delocalization transition is the point where f changes sign from negative to positive, as discussed earlier. Actually, to be more precise, the delocalization transition occurs when $f = -(\ln \mathcal{V})/L$ for finite L , when the translational entropy starts to exceed the binding energy. In the limit of large L we can say that the transition is at $f = 0$. We observe that the delocalization transition occurs at $v = 0.0478$ which is close to the value of g . We also observe that $m \ll w$ for $v \ll g$ and $m \gg w$ near the transition. Also for small v , $m \sim Y$, whereas near the transition $m \sim Y^2$. If we compare the value of w from Table I with the value of $L_m = 1/(2vG(Y^3))$ we find that w is smaller than L_m in the entire range. The ratio w/L_m varies from ~ 0.4 to 1 as v changes from 10^{-5} to 0.048. Thus the assumption we have made previously concerning this ratio is justified *a posteriori*.

Luckily it was possible to solve the minimization equations analytically almost entirely in both the limits $v \ll g$, and near the transition when $f \approx 0$. Details of the solutions are given in the Appendix of Ref. [35]. Here we only display the results:

A. The case $v \ll g$.

The parameters are given by

$$Y = \frac{2}{v}(\ln Y - 1)^{-1/2}(\ln Y + 3)^{-3/2}, \quad (108)$$

$$m = \frac{2}{3vg \ln Y}(\ln Y - 1)^{-1}(\ln Y + 3)^{-1}, \quad (109)$$

$$w = \frac{2}{3vg \ln Y}(\ln Y + 3)^{-1} \quad (110)$$

$$f = -9g^2(\ln Y)^2(\ln Y - 1)(\ln Y + 3)^{-1}. \quad (111)$$

| v | Y | m | w | f |
|---------|------|--------|-------|------------|
| 0.00001 | 2206 | 2413 | 16178 | -0.835249 |
| 0.0001 | 346 | 534 | 2580 | -0.421023 |
| 0.001 | 60 | 148 | 461 | -0.164673 |
| 0.01 | 13.7 | 66 | 97 | -0.0370883 |
| 0.02 | 11.1 | 69.2 | 60.8 | -0.0156444 |
| 0.03 | 12.8 | 105.5 | 41.9 | -0.0056033 |
| 0.04 | 22 | 302.6 | 26.8 | -0.0009992 |
| 0.045 | 35.6 | 720.1 | 20.7 | -0.0001776 |
| 0.0478 | 69.4 | 2342.4 | 16.5 | 0 |
| 0.048 | 77 | 2800 | 16 | 0.00000725 |

Table 2

Parameters and free energy for the case $g=0.05$

The first equation can be easily solved numerically for Y for a given value of v and the result substituted in the other equations. Very good agreement is achieved with Table I for small values of v .

B. Solution near the delocalization transition.

Let us define the parameter

$$\kappa = \frac{4v}{3g}. \quad (112)$$

In terms of this parameter we have

$$Y = \frac{1}{v\kappa} \left(\frac{1 + \sqrt{1 + \kappa^2}}{\kappa} \right)^2, \quad (113)$$

$$m = \frac{1}{v^2\kappa^2} \left(\frac{1 + \sqrt{1 + \kappa^2}}{\kappa} \right)^3, \quad (114)$$

$$w = \frac{\kappa}{8v^2 \ln Y} = \frac{1}{2vG(Y^3)}. \quad (115)$$

The transition point is obtained by solving the equation

$$\frac{1 + \sqrt{1 + \kappa^2}}{\kappa} + \frac{\kappa}{1 + \sqrt{1 + \kappa^2}} + \frac{1}{\kappa} \left(1 - 2 \ln \left(\frac{2(1 + \sqrt{1 + \kappa^2})}{\sqrt{3g\kappa^2}} \right) \right) = 0. \quad (116)$$

Once the solution κ_c is determined for a given g , then the transition point v_c is determined from $v_c = 3g\kappa_c/4$. For g in the range 0.01-0.2 we find that κ_c is a number of order unity (varies from 1.7 to 0.96 as g changes in that range). This means that v_c is quite close to g . Once v_c is known, all the parameters Y, m and w at the transition are determined by the solution above. For $g = 0.05$ we get $\kappa_c = 1.2744$, and thus $v_c = 0.0478$ in excellent agreement with the minimization results from Table 2.

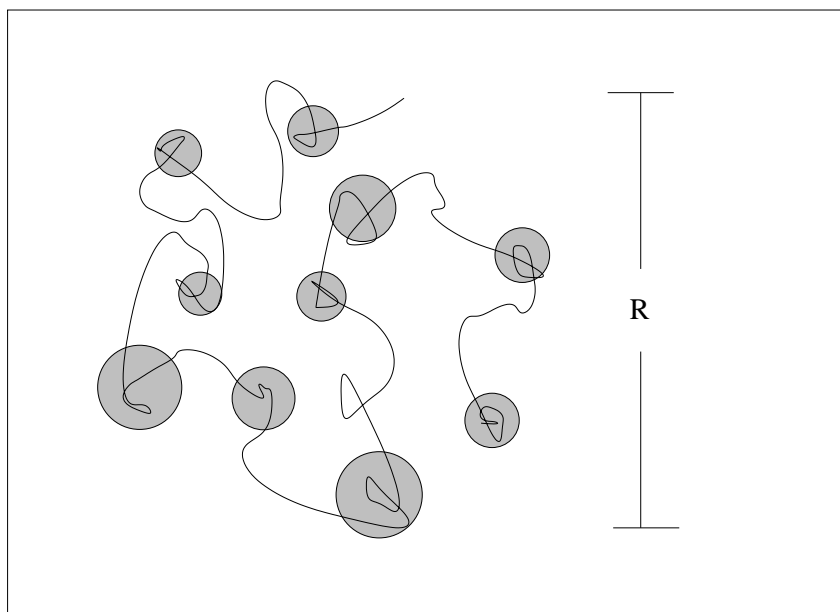


Figure 9. A typical chain conformation when $v \gg g$. The dark regions are regions of low average potential. Only short segments of the chain are situated in these regions.

For $v > v_c$ the chain is delocalized. The above expression for the free energy may no longer be accurate, but the general picture is clear. There will be very few monomers in the low regions of the potential, and the chain will behave very much like an ordinary chain with a self-avoiding interaction in the absence of a random potential. Any little perturbation can cause the chain to move to a different location in the medium (see Fig. (9)).

For small values of v when the chain is localized, we still expect its size to grow like that of a self-avoiding walk. Thus we expect roughly

$$R_g \sim YK^{0.6}, \quad (117)$$

since Y is the step size, and K is the number of steps. But since $K \approx L/(m+w)$ for large L , we find

$$R_g \sim \frac{Y}{(m+w)^{0.6}} L^{0.6}. \quad (118)$$

Thus the chain behaves as a self avoiding walk with an effective step size per monomer given by

$$\frac{a_{eff}}{a} = \frac{Y}{(m+w)^{0.6}}. \quad (119)$$

From Table 2 it becomes clear that the effective monomer size changes from a value of 6 for $v = 0.00001$ to a value of ~ 0.66 at the transition. The reason for the large value of

the effective monomer size at very small v is that the chains makes long jumps to take advantage of deep wells of the random potential, very much like anchored chains in a random potential that make sub-ballistic jumps [13]. This is also the reason why the number of monomers w in each well is somewhat less than L_m , since a sufficient number of monomers need to be used for the connecting segments. For $v \gg v_c$ in the delocalized phase we expect the effective monomer size to be about 1, since the chain behaves almost like an ordinary self-avoiding chain with the random potential not playing any significant role. Thus the chain is expected to have its smallest size in the vicinity of the transition.

It is important to notice that the discussion above is in the limit for very large L . If $L \lesssim 1/(2vG(\mathcal{V}))$, then in the localized phase when $v \ll v_c$ the polymer will be confined to a single well and will appear compact, even though it will not remain so for large L . This may explain why in simulations that were done typically with $L \leq 320$ [28] the delocalization transition appeared as a transition from a compact to a non-compact state of the polymer.

We should also note that for an annealed random potential there is a transition from a collapsed state into an ordinary self-avoiding chain as v increases through the point $v = g$ [11]. This is because the annealed free energy reads

$$F(R) = \frac{L}{R^2} - \frac{gL^2}{R^3} + \frac{vL^2}{R^3} + \frac{R^2}{L}. \quad (120)$$

For $v < g$ the fourth term is negligible and the free energy is lowest when $R \rightarrow 0$ (when L is large). For $v > g$ the first term is negligible, and the radius of gyration grows like

$$R \sim (v - g)^{1/3} L^{3/5}. \quad (121)$$

4.2. A self avoiding chain in a sea of hard obstacles

We now turn to the case of hard obstacles. This case of was discussed at length in the previous section in the absence of a self-avoiding interaction. We will make use of the results applicable to three spatial dimensions. Three different behaviors were identified as a function of the system's volume. Region I is defined when the system's volume $\mathcal{V} < \mathcal{V}_1 \sim \exp(c_1/\sqrt{x})$, where c_1 is a constant of order unity. Here $0 < x < 1$ is the average concentration of obstacles per site (total number of obstacles divided by total number of sites). We also assume that x is less than the percolation threshold ($x_c = 0.3116$ for a cubic lattice), so sites occupied by obstacles don't percolate. In Region I we recall from the previous section that in the absence of a self-avoiding interaction, the free energy per site for a chain situated in a spherical region of volume R^3 in three dimensions is given by

$$F_I/L = -\ln(z) + 1/R^2 + \hat{x} \quad (122)$$

where \hat{x} is the actual concentration of obstacles in that region, whose minimal expected value in a system of total volume \mathcal{V} is

$$\hat{x}_m \simeq x - \sqrt{\frac{x \ln \mathcal{V}}{R^3}}. \quad (123)$$

The binding energy per monomer inside the blob resulting from the lower concentration of obstacles in this region is given by $x - \hat{x}$, since it is equal the entropy gain from a lower

concentration as compared to the average (background) concentration x . The chain is “sucked” towards regions with low concentration of obstacles since it can maximize its entropy there, and these regions of space act like the negative potential regions of the Gaussian random potential. Thus in order for the free energy per monomer to reflect correctly the binding energy of the chain inside the blob, both the constant x of the background and the constant term $-\ln(z)$, which is always there regardless of the chain’s position, have to be subtracted. The relevant free energy per monomer situated in the blob (which is equal to minus the binding energy) is given by

$$f_I = \frac{1}{R^2} - \sqrt{\frac{x \ln \mathcal{V}}{R^3}}. \quad (124)$$

This result coincides with Eq. (23) upon the substitution $g \rightarrow x$. Thus all the results of the previous section carry on to Region I with this simple substitution .

Therefore we are going to discuss the situation when the system’s volume is greater than \mathcal{V}_1 (Region II). In this case the many blob picture still holds, where the blobs are now situated in regions free of obstacles (with $\hat{x} = 0$) whose size is determined again by the distance Y of the jump which is also assumed to satisfy $Y^3 \gtrsim \mathcal{V}_1$ (an assumption which will be justified *a posteriori*). In this case the farther the jump, it is more likely for the chain to find a larger space empty of obstacles, which will reduce further its confinement entropy w/R^2 and also the self-avoiding energy (but there is a cost resulting from the connecting segments and the constraint of the total length being fixed). The blob size is given by $R_{mII} = 1/G_o$ (the largest expected empty region in a volume Y^3) with [31]

$$G_o(Y^3) \approx \left(\frac{x}{3 \ln Y} \right)^{1/3}. \quad (125)$$

Thus the free energy per monomer of a chain consisting of a number of blobs with connecting parts, each of length Y , is given by

$$f(w, m, Y) \approx \frac{1}{w + m} \left(\frac{Y^2}{m} + \frac{m}{Y^2} + \frac{vm^2}{Y^3} - w(x - G_o(Y^3)^2) + vw^2 G_o(Y^3)^3 \right), \quad (126)$$

where again the constant x , which is independent of m , w and Y , has been subtracted. This assures that the delocalization transition again occurs at $f = 0$ and not at $f = x$. The results of a numerical minimization of this free energy is displayed in Table 3 for the case of $x = 0.1$.

The transition occurs between $v = 0.041$ and 0.042 . Again we could find analytically almost the entire solution both for $v \ll x$ and at the transition. The solution is given in the Appendix. There we show that the transition occurs at $v = 0.04142$. We observe that as for the case of a Gaussian random potential the ratio w/m changes from $\gg 1$ to $\ll 1$ as v approaches the transition from below. The values of Y are seen to be consistent with the assumption $Y^3 \gtrsim \mathcal{V}_1$. We also checked that the free energy from Table II is lower than what one would obtain by constraining Y to be in Region I, i.e. $Y^3 < \mathcal{V}_1$.

Finally for $\mathcal{V} > \mathcal{V}_2$, where $\mathcal{V}_2 \simeq \exp(x^{2/(d+2)} L^{d/(d+2)})$ (Region III), we expect the behavior of the chain to stay the same. This is because for jumps within a volume \mathcal{V}_2 the situation reverts to the previously discussed scenario, since the effective volume of interest

| v | Y | m | w | f |
|---------|-----|-------|-------|------------|
| 0.00001 | 552 | 2206 | 72092 | -0.062 |
| 0.0001 | 127 | 565 | 9135 | -0.051 |
| 0.001 | 38 | 206 | 1241 | -0.034 |
| 0.01 | 23 | 230 | 207 | -0.0077 |
| 0.02 | 32 | 536 | 137 | -0.0019 |
| 0.03 | 59 | 1737 | 120 | -0.00035 |
| 0.04 | 194 | 13915 | 131 | -0.0000099 |
| 0.041 | 248 | 21327 | 134 | -0.0000023 |
| 0.042 | 357 | 39310 | 144 | 0.0000024 |

Table 3

Free energy and parameters for a polymer in a sea of blockers when $\mathcal{V} > \mathcal{V}_1$.

which determines the statistics of the free spaces is of order Y^3 and we don't expect Y to be that large.

An important point to note is that if one performs a simulation with strict self-avoiding-walks on a diluted lattice (with $x < 1$), one has $v \sim 1$, and hence one will always be in the delocalized phase and will not see any localization effects [37].

A few words are in order about the case of an annealed potential. This case has been already investigated in the literature [34], and we will review it briefly. The free energy in the annealed case reads (for $d = 3$)

$$F(R) \approx \frac{L}{R^2} + xR^3 + \frac{vL^2}{R^3}. \quad (127)$$

The second term represents the entropy cost of a fluctuation in the density of obstacles that creates an appropriate spherical region of diameter $\sim R$. It was assumed that the chain occupies a spherical volume, or at least deviations from a spherical shape are not large [34]. In the case $v = 0$ one obtains by minimizing the free energy that $R \sim (L/x)^{1/5}$, a well known result. For $v > 0$ the first term is irrelevant (and so is the ‘‘stretching term’’ of the form R^2/L) and one finds that $R \sim (v/x)^{1/3}L^{1/3}$. In d dimension, the size scales like $L^{1/d}$ when $v > 0$, which is larger than the $L^{1/(d+2)}$ dependence in the $v = 0$ case. There is no indication for a phase transition in these arguments, although some authors [34] speculate that it breaks down for large v and a transition to a Flory $L^{3/(d+2)}$ dependence takes place.

5. Conclusions

In this chapter we have demonstrated the rich behavior of polymer chains embedded in a quenched random environment. As a starting point, we considered the problem of a Gaussian chain free to move in a random potential with short-ranged correlations. We derived the equilibrium conformation of the chain using a replica variational ansatz, and highlighted the crucial role of the system's volume. A mapping was established to that of a quantum particle in a random potential, and the phenomenon of localization was explained in terms of the dominance of localized tail states of the Schrödinger equation.

We also gave a physical interpretation of the 1-step replica-symmetry-breaking solution, and elucidated the connection with the statistics of localized tail states. Our conclusions support the heuristic arguments of Cates and Ball, but it starts with the microscopic model.

We then proceeded to discuss the more realistic case of a chain embedded in a sea of hard obstacles. Here, we showed that the chain size exhibits a rich scaling behavior, which depends critically on the volume of the system. In particular, we showed that a medium of hard obstacles can be approximated as a Gaussian random potential only for small system sizes. For larger sizes a completely different scaling behavior emerges.

Finally we considered the case of a polymer with self-avoiding (excluded volume) interactions. In this case it was found that when disorder is present, the polymer attains the shape like that of a pearl necklace, with blobs connected by straight segments. Using Flory type free energy arguments we analyzed the statistics of these conformational shapes, and showed the existence of localization-delocalization transition as a function of the strength of the self-avoiding interaction.

The work described in this chapter is concerned with static (equilibrium) properties of polymers in random media. There is a lot of theoretical work still to be done related to the dynamics, and especially nonequilibrium properties of polymers in random media. This is also of practical importance, for example for the separation of chain of different length or mass like DNA molecules under the effect of an applied force when embedded in a random medium like a gel [38].

6. Acknowledgments

This work was supported by the US Department of Energy (DOE), Grant No. DE-FG02-98ER45686.

REFERENCES

1. G. Guillot, L. Leger and F. Rondelez, *Macromolecules* **18**, 2531 (1985).
2. M.T. Bishop, K.H. Langley, and F. Karasz, *Phys. Rev. Lett.* **57**, 1741 (1986).
3. L. Liu, P. Li, and S.A. Asher, *Nature (London)* **397**, 141 (1999); L. Liu, P. Li, and S.A. Asher, *J. Am. Chem. Soc.* **121**, 4040 (1999).
4. J. Rousseau, G. Drouin, and G.W. Slater, *Phys. Rev. Lett.* **79**, 1945 (1997).
5. D.S. Cannell and F. Rondelez, *Macromolecules* **13**, 1599 (1980).
6. M. Doi and S. F. Edwards, *The Theory of Polymer Dynamics* (Oxford University Press, Oxford, 1986).
7. R. P. Feynman, *Statistical Mechanics: A Set of Lectures* (Benjamin, New York, 1972).
8. Y. Y. Goldschmidt, *Phys. Rev. E* **53**, 343 (1996).
9. D. R. Nelson and V. M. Vinokur, *Phys. Rev. B* **48**, 13060 (1993).
10. Y. Y. Goldschmidt, *Phys. Rev. B* **56**, 2800 (1997).
11. T. Nattermann and W. Renz, *Phys. Rev. A* **40**, 4675 (1989).
12. W. Ebeling, A. Engel, B. Esser and R. Feistel, *J. Stat. Phys.* **37**, 369 (1984).
13. M. E. Cates and C. Ball, *J. Phys. (France)* **89**, 2435 (1988).
14. P. G. de Gennes, *Scaling Concepts in Polymer Physics*. Cornell Univ. Press, Ithaca (1979).

15. S. F. Edwards and M. Muthukumar, *J. Chem. Phys.* **89**, 2435 (1988).
16. P. W. Anderson, *Phys. Rev.* **109**, 1492 (1958).
17. B. Souillard, in *Chance and Matter, Proceedings of the Les Houches Lectures, 1986*, Eds. J. Souletie, J. Vannismenus, and R. Stora (North-Holland, Amsterdam, 1987)
18. J. Fröhlich and T. Spencer, *Commun. Math. Phys.* **88**, 151 (1983).
19. I. M. Lifshitz, S.A. Gredeskul, and L.A. Patur, *Introduction to the Theory of Disordered Systems* (Wiley, NY, 1988); I. M. Lifshits, *adv. Phys.* **13**, 483 (1964).
20. Y. Shiferaw and Y. Y. Goldschmidt, *Phys. Rev. E* **63** 051803 (2001).
21. M. Mezard, G. Parisi and M. A. Virasoro, *Spin glass theory and beyond* (World Scientific, Singapore, 1987).
22. Y. Y. Goldschmidt, *Phys. Rev. E* **61**, 1729 (2000).
23. E. I. Shakhnovich and A. M. Gutin, *J. Phys. A* **22**, 1647, (1989).
24. M. Mezard and G. Parisi, *J. Phys. I France* **1**, 809 (1991).
25. W. H. Press *et al.*, *Numerical Recipes in Fortran*, 2nd ed. (Cambridge University Press 1992).
26. J. P. Bouchaud and M. Mezard, *J. Phys. A: Math. Gen.*, **30** (1997) 7997.
27. B. Halperin, *Phys. Rev.* **139**, A104 (1965).
28. A. Baumgartner and M. Muthukumar, *J. Chem. Phys.* **87**, 3082 (1987); see also review chapter by these authors in *Advances in Chemical Physics (vol. XCIV) Polymeric Systems* I. Prigogine and S. A. Rice editors, (John Wiley & Sons, Inc., New York, 1996) and references therein.
29. K. Leung and D. Chandler, *J. Chem. Phys.* **102** (3), 1405, (1995) ; D. Wu, K. Hui, D. Chandler, *J. Chem. Phys.* **96** (1), 835, (1992).
30. J. Dayantis, M.J.M. Abadie, and M.R.L. Abadie *Computational and Theoretical Polymer Science*, Vol. 8, 273 (1998).
31. Y.Y. Goldschmidt and Y. Shiferaw, *Eur. Phys. J. B* **25**, 351 (2002)
32. W. Feller, *An Introduction to Probability and its Applications*. Wiley, New York, 1963.
33. J. M. Luttinger in *Path Integrals and their Applications in Quantum, Statistical, and Solid State Physics*, G. J. Papadopoulos and J. T. Devreese editors. (Plenum Press, New York, 1978).
34. J. D. Huneycutt and D. Thirumalai, *J. Chem. Phys.* **90**, 4542 (1989).
35. Y. Y. Goldschmidt and Y. Shiferaw, *Eur. Phys. J. B.* **32**, 87 (2003).
36. C. Domb and G. S. Joyce, *J. Phys. C* **5**, 956 (1972).
37. K. Barat and B. K. Chakrabarti, *Phys. Rep.* 258, 377 (1995).
38. Jean-Louis Viovy, *Rev. Mod. Phys.* **72**, 813 (2000).